Deformed Shapes of Structures equipped with Viscous Dampers

A. Lago
Skidmore, Owings and Merrill LLP, San Francisco, USA, Formerly ROSE School, Pavia

T.J. Sullivan
University of Pavia, Pavia, Italy

G.M. Calvi
IUSS Pavia, Pavia, Italy

SUMMARY:
It is common practice to assume that viscous damping devices do not influence the deformed shapes of structures for excitation frequencies less than 4Hz. This study investigates the validity of this assumption for different structural configurations and damper distributions. Non-linear time-history (NLTH) analyses are carried out in order to verify the influence of viscous dampers on reinforced concrete moment resisting frames (MRF) and wall structures. Results show that deformed shapes of MRFs are more influenced by damper configurations than walls. In particular, when dampers are provided only in selected floors the response is difficult to predict due to several factors. In light of these findings, some approximate relationships are proposed to better estimate the deformed shapes of such structures. The results of NLTH analyses indicate that, compared to current design approaches, the new expressions can provide much improved prediction of the system response.

Keywords: displacement shape, viscous damper, displacement-based design, damper location.

1. INTRODUCTION

In the past several decades the application of passive added damping devices as a means for more reliable and safer design of structures in seismic regions, has steadily increased; even if, the research conducted in this field has not yet lead to standardized design procedures. Consequently, the majority of buildings codes, while allowing for the utilization of damper devices, do not provide any guidelines for their design. In light of this, a number of researchers (Lin et al. 2003, and Sullivan and Lago 2012, Lago *et al*. 2012) have been developing the direct displacement-based design (DDBD) approach of Priestley *et al*., (2007). Starting from these proposals for DDBD, this paper investigates the influence of damper positions within a structure. Indeed, in most of the cases it is common practice to assume that viscous dampers do not introduce any stiffness in a system for excitations greater than 4 Hz (Christopoulos and Filiatrault, 2006). Among all the different parameters that influence the response, the most important could be expected to be the amount of energy dissipated by the damping system and the distribution of dampers in the structure over the building height. All these aspects will be reviewed in this paper, with reference to results of a large number of NLTH analyses of different structural systems.

1.1 Viscous Damper Principles

The constitutive law of viscous dampers depends on the power of velocity exponent, α (Eqn.1.1):

$$f_D = C \operatorname{sgn}(\dot{u})|\dot{u}|^{\alpha} \tag{1.1}$$

where f_D is the damper force; $\dot{u}$ is the damper velocity; C is the damper constant; α is a real positive exponent with values that range between 0.1 to 1.0 for seismic applications (Asher *et al*., 1996); and sgn() is the sign function. Dampers are defined as linear (LVD) when $\alpha = 1$ and as non-linear (NLVD)

when $\alpha < 1$ (Fig. 1.1). This particular constitutive law is intrinsic to the behaviour of the damper device, since it is usually composed of a steel piston. This pushes oil through an orifice, in such a way that a pressure differential is created across the piston head. As a direct consequence, the fluid reduces its volume and being incompressible, develops a restoring force. This phenomenon can be prevented through the utilization of an accumulator and tests have shown that for motions less that 4Hz no remarkable stiffness is created (Christopoulos and Filiatrault, 2006). However, stiffening of higher modes could occur, since in this case the frequencies can be greater than 4Hz (Lago *et al*. 2012).
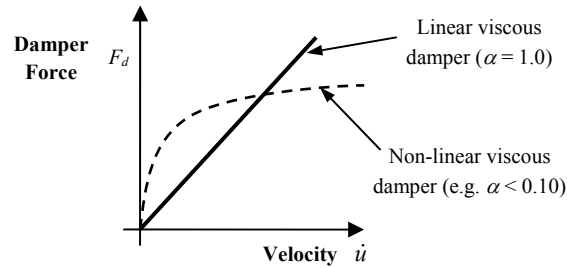

Figure 1.1. Force-velocity relationship for viscous dampers

2. SEISMIC DESIGN OF STRUCTURES WITH ADDED DAMPERS

The lack of detailed in current codes is perhaps a reflection of the limited number of research works available in the literature regarding the seismic design of building structures equipped with dampers. There appears to be even less guidance as how to proceed with the design of systems in which dampers are located on isolated floors. In light of this, recent research (Lin et al. 2003, Priestley et al. 2007, Sullivan 2009, Sullivan and Lago 2012, Lago *et al*. 2012) has been looking at the direct displacement-based seismic design of structures with added dampers. Before reviewing the latest recommendations, a brief overview of the DDBD approach will be provided with reference to Fig. 1.2.

The first two steps of the methodology (Fig. 1.2(a) and (b)) consist in finding the properties of the equivalent single degree of freedom system (effective mass, M_e, effective height, H_e, and design displacement, Δ_d). Subsequently, the designer has to defined the expected ductility demand at the design displacement, μ ($= \Delta_d / \Delta_y$, where Δ_y is the yield displacement), in order to set an equivalent viscous damping (Fig. 1.2(c)). This damping value accounts for the non-linear response of the structure and as a consequence the magnitude varies as a function of the structural system hysteretic properties (Priestley *et al*. 2007). Moreover, when using damping devices, an additional viscous damping source needs to be added to the total system viscous damping. The last step of the process is to scale the displacement response spectrum to the design equivalent viscous damping (Fig. 1.2(d)) and to compute the required effective period, T_e, from the design displacement. As a result, the effective period can be related to a required equivalent SDOF effective stiffness, K_e, from Eqn.2.1 and the design base shear from Eqn.2.2. Note that the base shear can be distributed over the building storeys as a series of equivalent lateral forces, F_i, to each level i, as shown in Eqn. 2.2.

$$K_e = 4\pi^2 \frac{m_e}{T_e^2} \tag{2.1}$$

$$V_b = K_{eff}\Delta_d \rightarrow F_i = V_b \frac{m_i \Delta_i}{\sum_{i=1}^{n} m_i \Delta_i} \tag{2.2}$$

where m_i is the seismic mass at level i, and Δ_i is the design displacement of level i. The base shear can also be increased to account for P-delta effects using the recommendations of Priestley et al. (2007).
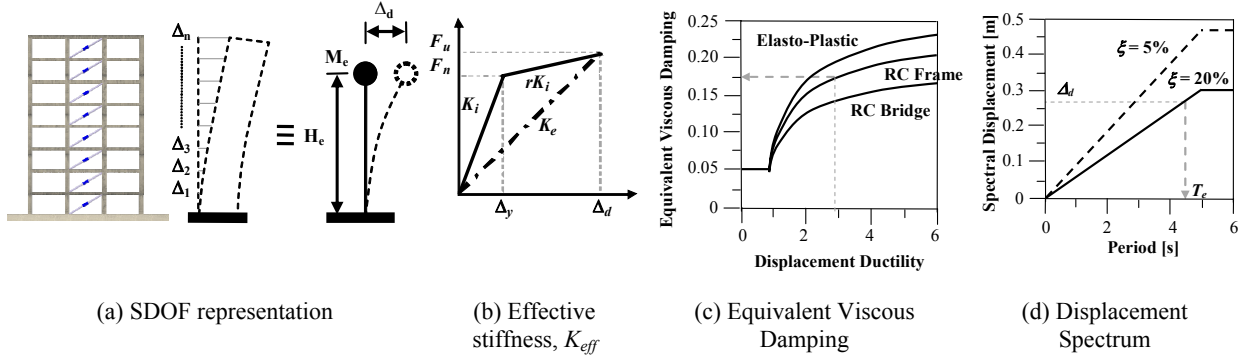
(a) SDOF representation   (b) Effective stiffness, K_{eff} (c) Equivalent Viscous Damping   (d) Displacement Spectrum

Figure 2.1. Fundamentals of DDBD (adapted from Priestley *et al*., 2007)

2.1 Design Assumptions

Having briefly reviewed the direct displacement-based design approach, some of the implications of introducing added damping devices will be reviewed:

- The energy dissipated by the added damping devices can be set or selected to be proportional to the stored strain energy in the bare structure (Fig. 2.2):

$$V_{Dam}\varDelta_D = \sum F_{di}\varDelta_{di} = \beta V_{Stru}\varDelta_d \tag{2.3}$$

where β is the strain energy constant of proportionality (the value of β is a designer choice, common values go up until 0.6), V_{Dam}, is the total damper base shear force, F_{di} is the damper force per floor and $\varDelta_{di}$ is the damper displacement. The summation term indicates the energy dissipated by the viscous dampers that can be simplified as the damper base shear, V_{Dam}, times the equivalent SDOF design displacement, $\varDelta_d$.
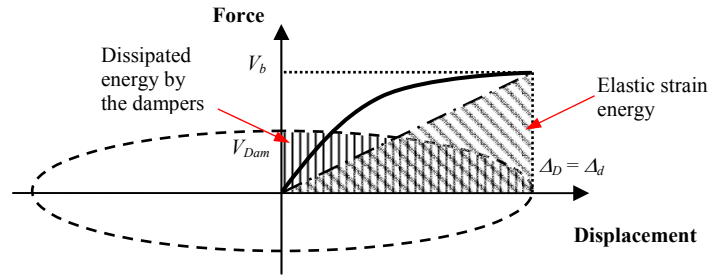

Figure 2.2. Strain energy constant of proportionality for systems with viscous dampers (Lago *et al*., 2012)

- The system viscous damping can be defined using the following base shear proportion (as proposed by Sullivan (2009) and updated by Lago *et al*. 2012):

$$\xi_{sys} = \frac{2V_{Stru}\xi_{Stru}\varDelta_d + V_{Dam}\varDelta_d}{2V_{Tot}\varDelta_d} = \frac{2V_{Tot}\xi_{Stru}\varDelta_d + \beta V_{Tot}\varDelta_d}{2V_{Tot}\varDelta_d} = \frac{2\xi_{Stru} + \beta}{2} = \xi_{Stru} + \frac{\beta}{2} \tag{2.4}$$

where ξ_{Stru} is the structural equivalent viscous damping constant of the system, given by the sum of the inherent (ξ_{in}) and the inelastic behaviour damping (ξ_{hy}).

- Having determined the required damper base shear, V_{Dam}, it is necessary to select a damper distribution that introduces the required equivalent viscous damping into the system. Lago et al. (2012) propose a means of permitting many different configurations, such as those shown in Fig. 2.3. The dampers distribution (along the building height), ϖ_i, is normalized against a chosen configuration:

$$C_{Di} = C_D \varpi_i \qquad\qquad (2.5)$$

where C_{Di} is the damper constant for the i-th floor and C_D is the reference damping constant. In this work, the following damper distributions are utilized (Fig. 2.3): (i) a *Constant* distribution in which equal damper properties are provided over the entire building; (ii) a *Beta* distribution in which damper constants are set to be proportional to the storey shear; (iii) a *bottom-half* (BH) distribution in which storeys over the bottom half of the building are equipped with uniform damper properties; (iv) a *top-half* (TH) distribution in which the upper half of the building is equipped with dampers; and (v) a series of localized distributions , in which only selected parts of the building (Fig. 2.3(c)) are equipped with viscous dampers of equal properties (*irj* notation, e.g. 2r4 means that the floors at the two quarter of the building (starting from the bottom) are equipped with dampers).
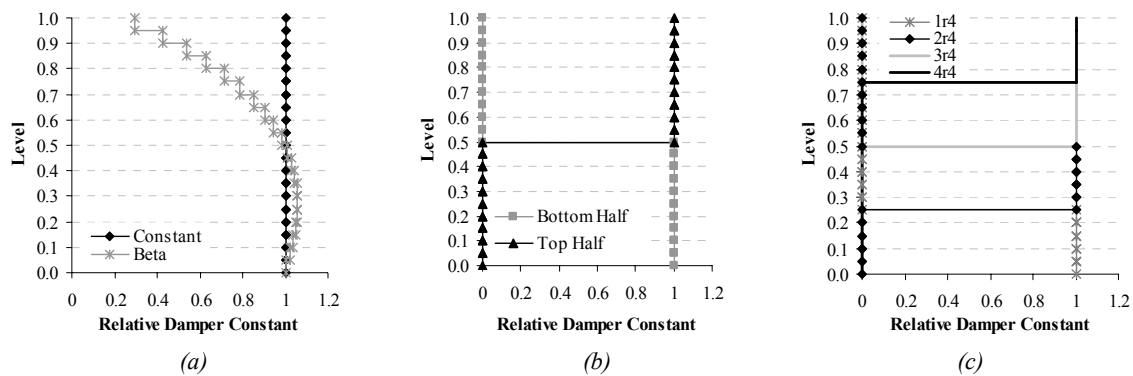

(a) *(b)* *(c)*

Figure 2.3. Damper distributions (modified from Lago *et al*. 2012)

3. NON-LINEAR TIME HISTORY ANALYSES

In order to gauge the ability of the proposed design approach to control the response of diverse structural systems, non-linear time history analyses have been carried out and in this section results will be reviewed. However, before moving to the NLTH discussion, the structural systems utilized are briefly described together with the record set considered (for a detailed review see Lago *et al*. 2012).

3.1 Structural Systems

The proposed design procedure is tested for two different structural systems: moment resisting frames (Fig. 3.1(a)) and structural walls (Fig. 3.1(b)). In the figure, it is shown that the approach is applied to systems equipped with diagonal braces, but the same procedure can be utilized for other damper configurations (e.g. toggle brace configuration) as shown in Lago *et al*. (2012). Several structural heights were studied in Lago *et al*. (2012), but in this paper only systems with 12 and 20 storeys are reviewed. These systems are designed for a drift limit of 2% implying that the systems behave inelastically.

3.2 Seismic Demand

The research considers the Eurocode 8 (CEN, 2004) type 1 spectrum constructed for a soil type C, a corner period of 8s and a PGA = 0.4g as shown in Fig. 3.2. A set of 10 records (from the PEER database) have been utilized throughout all these investigations and the relative acceleration and displacement spectra are also shown in Fig. 3.2 (for details of the record selection refer to Lago *et al*. 2012).
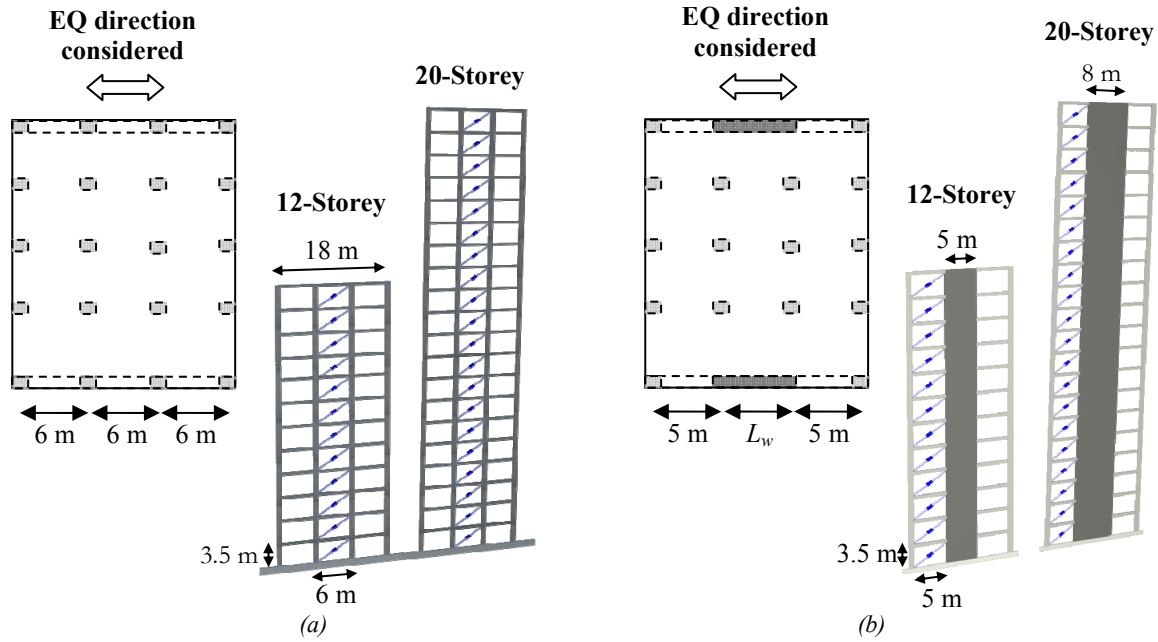
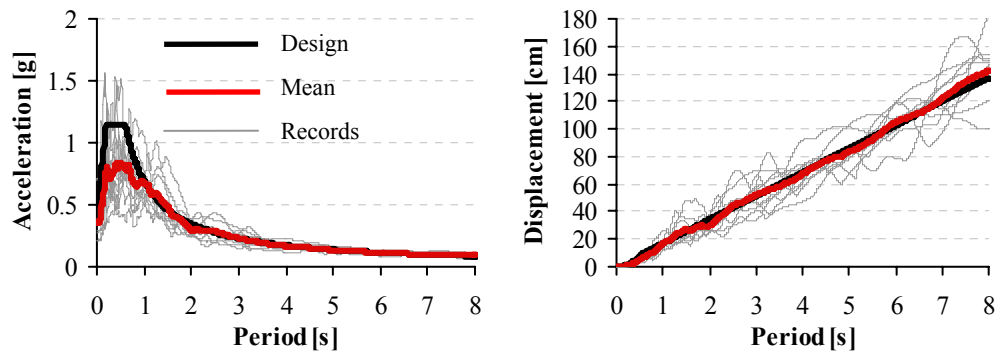**Figure 3.1.** RC-frame (a) and structural wall (b) with dampers in diagonal braces (Lago *et al*. 2012)

Figure 3.2. Ground motions for NLTHAs: (a) acceleration and (b) displacement spectra (Lago *et al*. 2012)

3.3 Sizing the Viscous Dampers

For each of the structural systems reviewed in Section 3.1, dampers were sized using the Direct DBD approach (Lago *et al*. 2012) for three different constants of proportionality (β = 0.2, 0.4 and 0.6) and two viscous damper typologies (linear, α = 1, and non-linear, α = 0.1). This lead to significantly different total sums of damper constants, as shown in Fig. 3.3, that vary with the structural system, structural height and damper distribution. The figure shows both the cases of linear and non-linear viscous dampers and it is important to note that similar trends can be found for the other parameter configurations (see Lago *et al*. (2012) for further details). The different designs for MRFs (Fig. 3.3(a,c)) show that the constant and beta distributions provide similar damper constant sums, while the BH distribution requires the smallest sum of damper constants. This is a consequence of the high drift (and consequently velocity) demands expected at the lower levels. Indeed, the situation is completely different for the TH distribution since at the upper storeys lower velocities are expected and as a result, higher damper constant sums are required to provide the same design level of energy dissipation. Similar trends are found for the localized distributions, in which the upper storey distributions require the greater sum of damper constants. Fig. 3.3(b,d) also shows the damper sum requirements for structural walls and it can be seen that the situation is the opposite to the MRFs, since for structural walls higher drift demands (and velocities) are expected at the top floors. Note that, similar trends were encountered for other building heights and for systems with NLVDs (Lago *et al*. 2012).
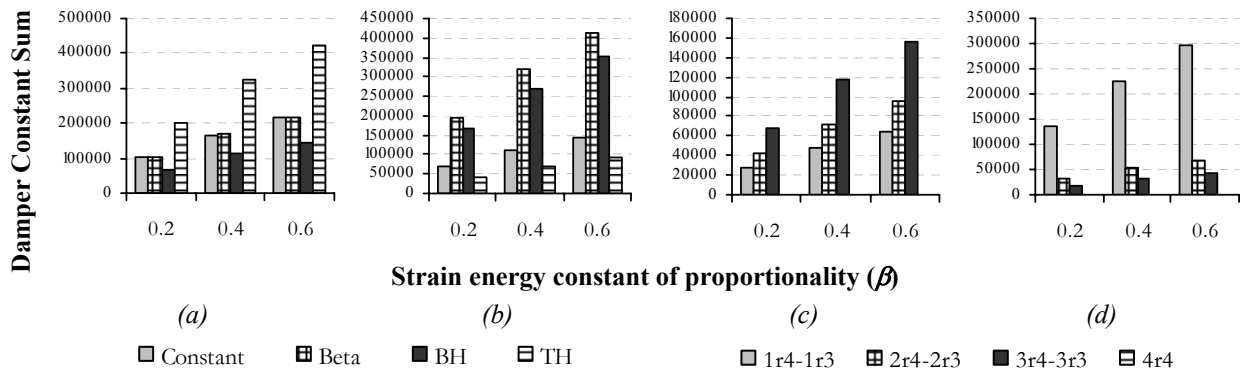
Figure 3.3. LVD total constants required for 12-storey MRFs (a, c) and RC walls (b, d) (Lago *et al.* 2012)

4. MOMENT RESISTING FRAMES

The previously designed MRF systems are subject to a series of NLTH analyses in Ruaumoko (Carr, 2011) using 10 spectrum-compatible records (see Fig. 3.2). For details of the lumped plasticity modelling and analysis approach, see Lago et al. (2012). The response of the structures is gauged by looking at the interstory drift, which can furnish insight on the demands on both the main structural systems and the added damping devices. Fig. 4.1 shows the response of the systems for different damper distributions and it can be seen that similar trends are developed for both LVDs and NLVDs. However, damping systems with NLVDs give more pronounced effects since the velocity power factor is very low ($\alpha = 0.1$) and as a consequence the dampers act almost in phase with the main structural system. This is the opposite of the behaviour of linear viscous damper ($\alpha = 1$), in which the maximum response of the dampers and the main structural system is almost completely out-of-phase (see Lago *et al.* (2012) for further details). Fig. 4.1 shows that the behaviour is well controlled when the dampers are inserted in each storey. Discrepancies with the design values become slightly evident for the taller structures. This highlights the need for a revised displacement shape assumption for MRFs, since the expression currently utilized in the Direct DBD (from Pettinga and Priestley, 2005) leads to overdamped storey drifts at the top levels (see Section 4.1.1).
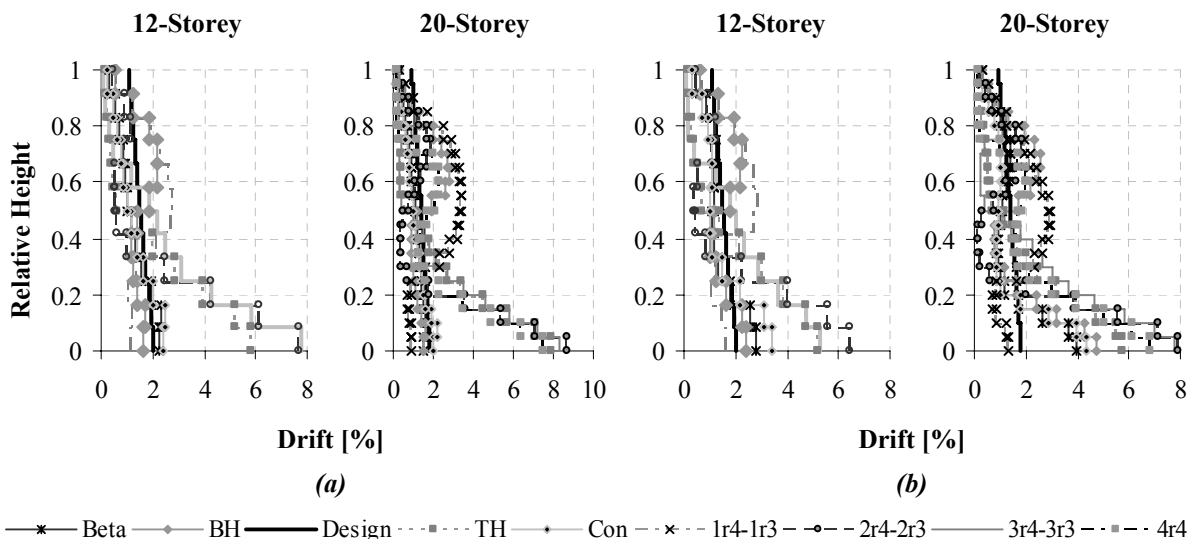

Figure 4.1. MRFs drift response with LVD (a, c) and NLVD (b, d) (Lago *et al.* 2012)

A completely different response is shown for the localized distributions of dampers, in which the floors not equipped with dampers experience very large drifts. Interestingly, when just the bottom storeys of the MRF building are equipped with viscous dampers the drift limit of 2% is only slightly

exceeded at the top floors. Instead, looking at the distributions in which the top floors are equipped with viscous dampers, the drift demands at the bottom storeys are excessive (up to 9%); while at the top storeys they are very small. This means that for MRF systems the positioning of dampers over lower storeys can provide reasonable control of the response, even if if might be necessary to enhance the response of the floors in which dampers are not applied (see Section 4.1.2).

4.1 Revised Design for Frame Structures with Viscous Dampers

In the previous sections, it was shown how the proposed method by Lago *et al.* (2012) permits the control of MRF system response in terms of drifts demands. However, the performance was not completely satisfactory and consequently a revised version of the design is herein proposed for different damper configurations.

4.1.1 Modified Displacement Profile for Non-linear Frames with Viscous Dampers
The NLTHA results (Fig. 4.1) highlighted the necessity to revise the current displacement profile definition when frame structures, equipped with viscous dampers, are behaving inelastically. In order to consider this behaviour, an updated version of the design profile is proposed (Eqn. (4.1)).

$$\Delta_i = \omega_\theta \theta_c H_i \frac{pH_n - H_i}{pH_n - H_1} \tag{4.1}$$

where H_i is the height of the *i*-th floor from the basement, n is the number of floors, θ_c is the critical storey drift and ω_θ is the reduction factor that accounts for higher mode effects (Priestley *et al.* 2007). The factor p is calibrated to the results of NLTH analyses and the original value was set to 4 (as reported by Pettinga and Priestley, 2005). However, to account for the behaviour highlighted in Fig. 4.1, the constant p should be optimized and a trial value of 2 is set. In order to gauge the capacity of the update displacement profile formulation, the previous case study structures have been re-designed and re-analyzed and the relative results are shown in Fig. 4.2. The modified design displacement profile enhances the performance greatly compared with the existing design profile (with $p = 4$). Therefore, it can be concluded that the updated profile allows more efficient control of the behaviour of inelastic MRF systems equipped with viscous dampers.
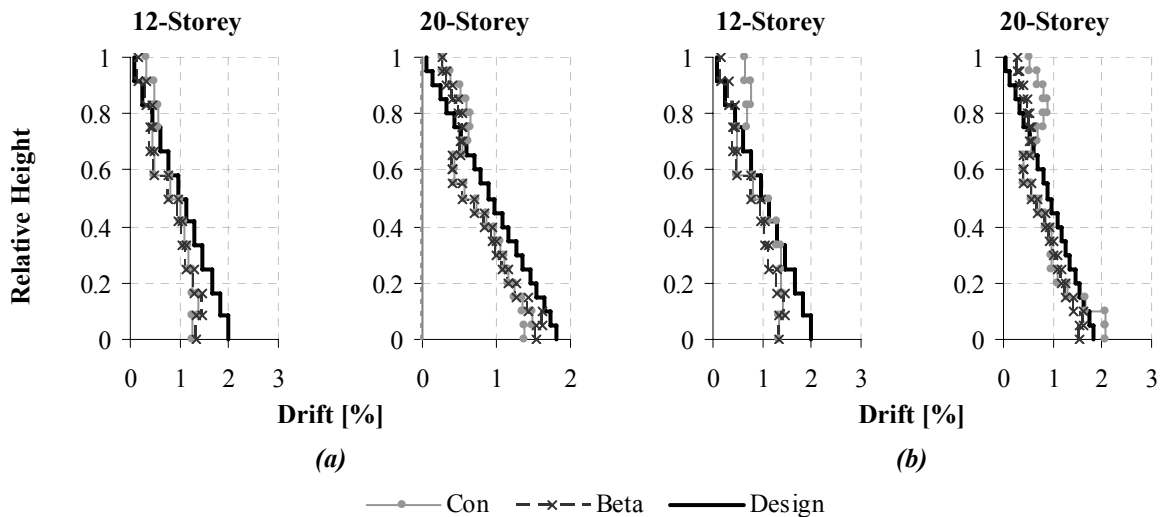

Figure 4.2. MRFs response with updated displacement profile: (a) LVDs and (b) NLVDs (Lago *et al.* 2012)

4.1.2 Strength Distribution for Frame Structures with Localized Dampers
In the previous sections it was shown that the structural response of MRF structures is greatly influenced by the localized damper distributions with drift concentrations tending to occur at storeys without dampers. Consequently, the design procedure needs to be improved if localised damper

distributions are to be permitted. One option could be to update the displacement profile of the system but when localized dampers are utilized this does not seem very practical, because the shears and moments demands are not uniformly distributed (as shown in Lago *et al*. 2012). Therefore, an alternative approach is considered in which the strength of the floors without dampers is increased. A simple way do this is to utilize the same properties coming from the DDBD of the bare structure (i.e. without dampers). Results shown earlier in Fig. 4.1 suggest that this solution could be effective because the response of the floors without dampers was close in shape to the undamped response case (see also Lago *et al*. 2012).

To investigate the feasibility of this new approach, the strength of the floors without dampers has been upgraded for the case study structures and NTLHAs were repeated to gauge the performance. Fig. 4.3 compares the peak drifts of the original and upgraded design solutions for structures equipped with LVDs and NLVDs with BH distribution. In both cases, the response of the upgraded system is more optimal, even if the upper storey drifts are conservatively low compared to the design values. Therefore, while the solution has been successful in enhancing the overall performance, it might not be optimal from an economical point of view. Therefore, more efficient strength distributions could be developed as part of future research.
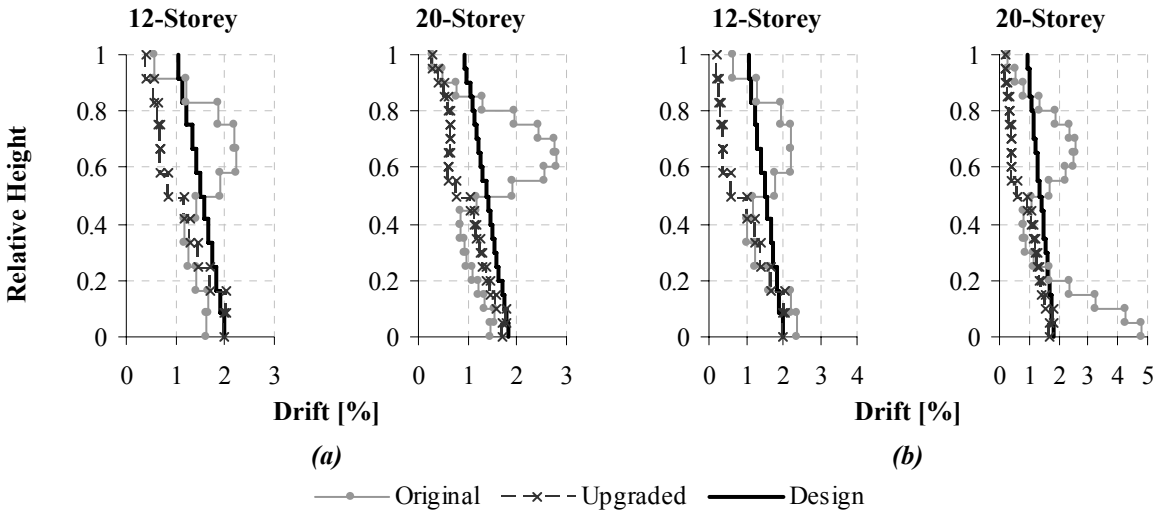

Figure 4.3. Response with updated strength for BH distribution: (a) LVDs and (b) NLVDs (Lago *et al*. 2012)

For the case that the MRFs are designed according to the 1r4 damper distribution (1r3 for the 12-storey), the upgraded results are compared with the original design results in Fig. 4.4. The results, at least for LVDs, indicate that idea of upgrading the strength of the floors where dampers are not provided could indeed provide an effective means of controlling the response, (see Lago *et al*. 2012 for results of other response parameters). However, while the revised solution for LVDs provides a more efficient response, surprisingly the NLVDs are not able to control the bottom storey drifts. Further investigations into the reasons for this behaviour, while interesting, are outside the scope of this paper and can instead be found in Lago *et al*. (2012).
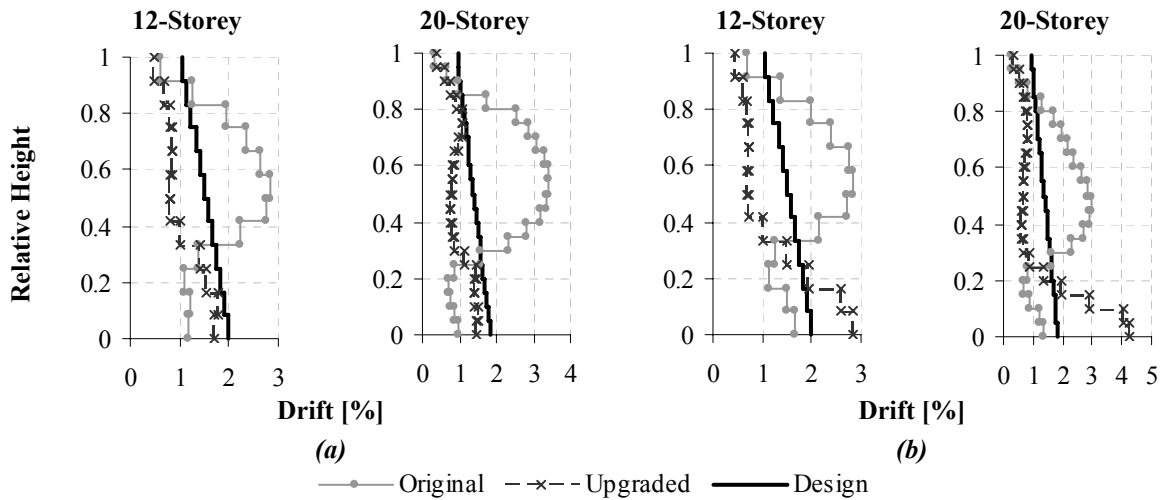
12-Storey **20-Storey** **12-Storey** **20-Storey**

(a) *(b)*

———•— Original – –×– – Upgraded ——— Design

Figure 4.4. Response with updated strength for 1r4 distribution: (a) LVDs and (b) NLVDs (Lago *et al*. 2012)

5. STRUCTURAL WALLS

The structural walls of Section 3 (Fig. 3.1) are also subject to a series of NLTH analyses in Ruaumoko (Carr, 2011) using 10 spectrum-compatible records (see Fig. 3.2). For details of the lumped plasticity modelling and analysis approach, see Lago et al. (2012). The response of the structures is again gauged by looking at the interstory drifts. Fig. 5.1 shows the response of the system for the different damper distributions.
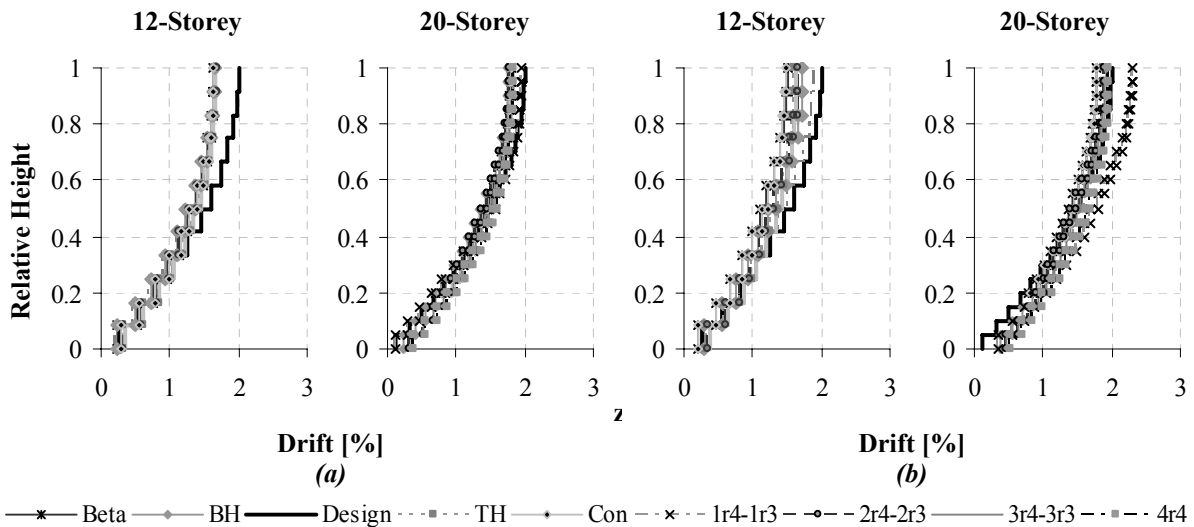

12-Storey **20-Storey** **12-Storey** **20-Storey**

(a) *(b)*

——×— Beta ——•— BH ——— Design · · ·■· · · TH —•— Con – ·×· – 1r4-1r3 –•– 2r4-2r3 ——— 3r4-3r3 – ·■– · 4r4

Figure 5.1. Structural walls drift response with LVD (a, c) and NLVD (b, d) (Lago *et al*. 2012)

The average results, for all the distributions, demonstrate the ability of the procedure to provide a design that effectively controls the response and the discrepancies with the design values are consistent with the record variability. In particular, all the configurations produce conservative results compared with the design solution, since the top storey drifts are in general smaller than the expected ones. The drift limit of 2% is satisfied in all cases and until the mid-height the response is very close to the design profile. Looking closely at the response for the different damper configurations, the drifts show that the localized top storey distributions do not effectively damp the bottom storey displacements (in relation with the design values); even if, the storeys drifts, at these levels, are well below the 2% limit. Comparing this design solution with the MRFs behaviour (Fig. 4.1), it is clear that the two systems respond very differently to the use of diverse damper configurations. Indeed, the

response of structural wall systems is not significantly influenced by the damper locations.

6. CONCLUSIONS AND FUTURE WORKS

This paper has investigated the design of structures with viscous dampers. The focus has been on the influence of damper locations on the structural response of both moment resisting frames and structural walls. The design was done in accordance with an innovative displacement-based design (DBD) procedure, based on the work carried by Lago *et al*. (2012) and Sullivan and Lago (2012). The NLTH results have shown that while the general DBD procedure works well when dampers are located at all floors, this is not the case when damper distributions are non-uniform. Indeed, the common assumption that dampers will not influence the structural displaced shape, has been shown to be inappropriate for MRF structures. On the contrary, the response of RC wall structures was fairly unaffected by damper positioning. As a consequence, an updated version of the displacement profile shape was proposed for frames responding inelastically with dampers at all floors. Numerical results illustrated improvements compared to the traditional DDBD solution. Furthermore, an alternative strength distribution for frame structures with localized damper distributions has been proposed, adjusting the displacement profile between floors with and without dampers. NLTHs results illustrated that the proposed procedure is very promising, even if further research is required in order to find more economical strength distributions.

All these results have highlighted that for moment resisting frames the optimal damper distributions may be those in which dampers are located over the lower stories, since they require the smallest sum of damper constants and lead to a better response in term of drift demands. Instead, for wall structures the opposite is true, with optimal solutions obtained when dampers are located over upper storeys. In closing, this work has highlighted the need for improved means of considering localized distributions of dampers in frame and arguably also in wall structures and this should be part of future research.

REFERENCES

Asher, J., Young, R.P., Ewing, R. (1996). Seismic isolation design of the San Bernardino county medical center replacement project," *Journal of Structural Design of Tall Buildings*, **5**, 265-279.

Calvi, G.M., Sullivan, T.J. (2012). A Model Code for the Displacement-Based Seismic Design of Structures, IUSS Press, Pavia, Italy.

Carr, A.J. (2011). Ruaumoko Software, University of Canterbury, Christchurch, New Zealand.

CEN (2004). Eurocode 8 –part 1: General rules, Seismic Actions and Rules for Buildings, European Committee for Standardization, Brussels.

Christopoulos, C., Filiatrault, A. (2006). Principles of Passive Supplemental Damping and Seismic Isolation, IUSS Press, Pavia, Italy.

Lago A., Sullivan, T.J., Calvi, G.M. (2012). Seismic Design of Structures with Passive Energy Dissipation Systems, IUSS Report, In press.

Lin, Y.Y., Tsai, M.H., Hwang, J.S. and Chang, K.C. (2003). Displacement-Based Design for Buildings with Passive Energy Dissipation Systems. *Engineering Structures, the Journal of Earthquake, Wind and Ocean Engineering*, **25:1**, 25-37.

Pettinga, J.D., Priestley, M.J.N. (2005). Dynamic behaviour of reinforced concrete frames designed with direct displacement-based design, IUSS Report, IUSS Press, Pavia, Italy.

Priestley, M.J.N, Calvi, G.M., Kowalsky, M.J. (2007). Displacement Based Seismic Design of Structures, IUSS Press, Pavia, Italy.

Priestley, M.J.N. (2003). Myths and fallacies in earthquake engineering, revisited, The ninth Mallet Milne Lecture, IUSS Press, Pavia, Italy.

Sullivan, T.J., Lago, A. (2012). Towards a simplified direct DBD procedure for the seismic design of moment resisting frames with viscous dampers, *Engineering Structures*, **35**, 140-148.

Sullivan, T.J. (2009) Direct displacement-based design of a RC wall-steel EBF system with added dampers, *Bulletin of the New Zealand Society for Earthquake Engineering*, **42:3**, 167-168.